

**DESULFURIZATION OF HYDROCARBON FEEDS BY  
II-COMPLEXATION ADSORPTION:  
CHARACTERIZATION OF COPPER HALIDES IMPREGNATED ON  
MESOPOROUS AND MACROPOROUS ALUMINAS**



Thanawat Aryusanil

A Thesis Submitted in Partial Fulfilment of the Requirements  
for the Degree of Master of Science  
The Petroleum and Petrochemical College, Chulalongkorn University  
in Academic Partnership with  
The University of Michigan, The University of Oklahoma,  
Case Western Reserve University, and Institut Français du Pétrole  
2011

**Thesis Title:** Desulfurization of Hydrocarbon Feeds by II-Complexation  
Adsorption: Characterization of Copper Halides Impregnated  
on Mesoporous and Macroporous Aluminas

**By:** Thanawat Aryusanil

**Program:** Petroleum Technology


**Thesis Advisors:** Asst. Prof. Pomthong Malakul  
Dr. Michel Thomas

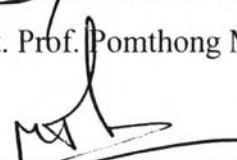
---


Accepted by the Petroleum and Petrochemical College, Chulalongkorn  
University, in partial fulfilment of the requirements for the Degree of Master of  
Science.

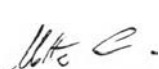
  
..... College Dean  
(Asst. Prof. Pomthong Malakul)

**Thesis Committee:**

  
.....  
(Asst. Prof. Pomthong Malakul)

  
.....  
(Dr. Michel Thomas)

  
.....  
(Asst. Prof. Siriporn Jongpatiwut)

  
.....  
(Assoc. Prof. Metta Chareonpanich)

**ABSTRACT**

5273025063: Petroleum Technology Program

Thanawat Aryusanil: Desulfurization of Hydrocarbon Feeds by  $\Pi$ -Complexation Adsorption: Characterization of Copper Halides Impregnated on Mesoporous and Macroporous Aluminas. Thesis Advisors: Asst. Prof. Pomthong Malakul and Dr. Michel Thomas  
158 pp.

Keywords: Activated alumina/ Adsorptive desulfurization/ Dispersing agent/ Impregnation/ Inverse gas chromatography (IGC)/  $\Pi$ -complexation

$\Pi$ -complexation sorbents have been developed for adsorptive desulfurization during the last decade. They were used to selectively remove organosulfur molecules from hydrocarbon feeds like diesel and gasoline. The  $\text{Cu}^+$  impregnated on mesoporous and macroporous aluminas adsorbents were studied. This research aimed to characterize these adsorbents with various methods, such as BET surface area analysis, particle density, structural density and pore volume analysis, Scanning Electron Microscopy (SEM), X-Ray Diffraction (XRD), Temperature-Programmed Reduction (TPR), Temperature-Programmed Desorption (TPD). To determine if there is a good adsorptive desulfurization, Inverse Gas Chromatography (IGC) was used to investigate. For IGC theory, there are stationary phase (non-impregnated alumina,  $\text{Al}_2\text{O}_3$ , and impregnated alumina,  $\text{Cu}/\text{Al}_2\text{O}_3$ ) and mobile phase (He). Normal alkanes ( $\text{C}_6$ – $\text{C}_{10}$ ) were used as probe molecules (as a reference), toluene and thiophene were used as polar probe molecules. The results expressed the distinction of surface properties between  $\text{Al}_2\text{O}_3$  and  $\text{Cu}/\text{Al}_2\text{O}_3$  by the specific interaction ( $I^{\text{sp}}$ ). The  $I^{\text{sp}}$  of toluene on m- $\text{Al}_2\text{O}_3$  at 200, 225 and 250 °C were 34.3, 32.9 and 31.8  $\text{mJ}/\text{m}^2$ , respectively, and on 30%  $\text{Cu}/\text{m-}\text{Al}_2\text{O}_3$  they were 29.2, 27.1 and 26.8  $\text{mJ}/\text{m}^2$ , respectively; and the  $I^{\text{sp}}$  of thiophene on m- $\text{Al}_2\text{O}_3$  were 61.8, 58.8 and 56.3  $\text{mJ}/\text{m}^2$ , respectively and on 30%  $\text{Cu}/\text{m-}\text{Al}_2\text{O}_3$  were 57.1, 56.1 and 56.0  $\text{mJ}/\text{m}^2$ , respectively.  $\text{Cu}/\text{m-}\text{Al}_2\text{O}_3$  has shown to be better in selective removal of organosulfur molecules than  $\text{Al}_2\text{O}_3$ .

## บทคัดย่อ

ธนวรรษ อายุชนะนิล : การกำจัดสารประกอบกำมะถันจากสารประกอบไฮโดรคาร์บอน โดยกระบวนการดูดซับด้วยพันธะไพ: การวิเคราะห์ตัวดูดซับที่ถูกทำให้ชุ่มด้วยสารละลายเกลือคลอไรด์ของคอปเปอร์บนอะลูมินาที่มีรูพรุนขนาดกลางและขนาดใหญ่ (Desulfurization of Hydrocarbon Feeds by  $\Pi$ -Complexation Adsorption: Characterization of Copper Halides Impregnated on Mesoporous and Macroporous Aluminas) อ. ที่ปรึกษา : ผศ. ดร. ปมทอง มาลากุล ณ อยุธยา ดร. มิเชล โทมัส 158 หน้า

ในช่วงทศวรรษที่ผ่านมา ได้มีการพัฒนาตัวดูดซับสำหรับการกำจัดสารประกอบกำมะถัน โดยกระบวนการดูดซับด้วยพันธะไพ ซึ่งตัวดูดซับเหล่านี้ถูกนำมาใช้ในการกำจัดสารประกอบกำมะถันอย่างเฉพาะเจาะจงจากสารประกอบไฮโดรคาร์บอนจำพวกน้ำมันดีเซลและแก๊สโซลีน การวิจัยนี้ทำการศึกษาตัวดูดซับที่ถูกทำให้ชุ่มด้วยสารละลายเกลือคลอไรด์ของคอปเปอร์บนอะลูมินาที่มีรูพรุนขนาดกลางและขนาดใหญ่ ซึ่งถูกนำมาวิเคราะห์ด้วยหลายวิธีการ ได้แก่ การวิเคราะห์พื้นที่ผิวแบบ B.E.T. การวิเคราะห์ความหนาแน่นและปริมาตรรูพรุน การวิเคราะห์ด้วย Scanning Electron Microscopy (SEM), X-Ray Diffraction (XRD), Temperature-Programmed Reduction (TPR) และ Temperature-Programmed Desorption (TPD) นอกจากนี้ ยังทำการวิเคราะห์ความสามารถในการดูดซับสารประกอบกำมะถันด้วยวิธี Inverse Gas Chromatography (IGC) ซึ่งประกอบด้วยสถานะที่อยู่หนึ่ง คือ ตัวดูดซับที่ถูกทดสอบ (ตัวดูดซับอะลูมินาก่อนและหลังทำให้ชุ่มด้วยสารละลายเกลือคลอไรด์ของคอปเปอร์) และสถานะที่เคลื่อนที่ (แก๊สฮีเลียม) ในการวิเคราะห์หาค่ามาตรฐานจะใช้แอลเคน ( $C_6-C_{10}$ ) เป็นโมเลกุลตรวจสอบแบบไม่มีขั้ว และใช้โทลูอินและไทโอฟินเป็นโมเลกุลตรวจสอบแบบมีขั้ว งานวิจัยนี้ใช้ค่าอันตรกิริยาจำเพาะในการแยกแยะคุณสมบัติของพื้นผิวตัวดูดซับเพื่ออธิบายความสามารถในการกำจัดสารประกอบกำมะถันที่แตกต่างกัน ค่าอันตรกิริยาจำเพาะระหว่างโทลูอินกับอะลูมินาที่อุณหภูมิ 200, 225 และ 250 °C คือ 34.3, 32.9 และ 31.8  $\text{mJ/m}^2$  ตามลำดับ และระหว่างโทลูอินกับอะลูมินาที่ถูกทำให้ชุ่ม (30% monolayer) มีค่าเท่ากับ 29.2, 27.1 และ 26.8  $\text{mJ/m}^2$  ตามลำดับ ส่วนระหว่างไทโอฟินกับอะลูมินา มีค่าเท่ากับ 61.8, 58.8 และ 56.3  $\text{mJ/m}^2$  ตามลำดับ และระหว่างไทโอฟินกับอะลูมินาที่ถูกทำให้ชุ่ม (30% monolayer) คือ 57.1, 56.1 และ 56.0  $\text{mJ/m}^2$  ตามลำดับ ผลการศึกษาแสดงให้เห็นว่า ตัวดูดซับอะลูมินาที่ถูกทำให้ชุ่มมีความสามารถในการกำจัดสารประกอบกำมะถันได้ดีกว่าตัวดูดซับอะลูมินาที่ไม่ถูกทำให้ชุ่ม

## ACKNOWLEDGEMENTS

I would like to sincerely express my thanks and gratitude to the following people and organization. Without their help, this thesis could not be very fruitful.

First of all, I would sincerely like to thank my advisors, Asst. Prof. Pomthong Malakul and Dr. Michel Thomas, for their help and guidance on a day to day basis during my doing research at the Petroleum and Petrochemical College and IFP Energies nouvelles. I would really appreciate their advice, suggestions, and comments.

I would like to give special thanks to Mr. Patrick Peslerbe, Ms. Christine Bounie, Ms. Sandra Montpeyrroux, Ms. Sophie Drozd, and Ms. Michèle Maricar-Pichon for their kind during my work at IFP Energies nouvelles.

I would really appreciate Asst. Prof. Siriporn Jongpatiwut and Assoc. Prof. Metta Chareonpanich, for kindly serving on my thesis committee.

I would also like to thank all my professors for their experience through their courses, giving me a chance to get knowledge about my thesis.

I am grateful for the scholarship and funding of the thesis work provided by the Petroleum and Petrochemical College; and the National Center of Excellence for Petroleum, Petrochemicals, and Advanced Materials, Thailand, and I would also like to express my special thank to EGIDE for financial support during conducting my research in France.

Thanks to all of staffs in PPC, the IFP Energies nouvelles's technicians and all the graduate students at PPC, who helped me over the year.

Thanks to all friends in Thailand and France, without their help and friendship, my beautiful experience in France can not complete.

Finally, special thanks to my family who always stand beside me in every moment. Without their support this thesis would not have been possible.

## TABLE OF CONTENTS

	<b>PAGE</b>
Title Page	i
Abstract (in English)	iii
Abstract (in Thai)	iv
Acknowledgements	v
Table of Contents	vi
List of Tables	ix
List of Figures	xi
<b>CHAPTER</b>	
<b>I INTRODUCTION</b>	<b>1</b>
<b>II LITERATURE REVIEW</b>	<b>3</b>
2.1 Crude Oil	3
2.1.1 Hydrocarbon in General	3
2.1.2 Composition of Crude Oil	3
2.2 Petroleum Fractions and Products	7
2.3 Hydrocarbon Feeds and Sulfur Specifications	12
2.4 Organosulfur Compounds	15
2.4.1 Hydrogen Sulfide	15
2.4.2 Mercaptans	15
2.4.3 Sulfides	16
2.4.4 Thiocyclic Compounds	16
2.5 Desulfurization Process	20
2.5.1 Conventional Hydrodesulfurization (HDS)	22
2.5.2 Challenges of Ultra Deep Desulfurization	23
2.5.3 Developing New Processes	34
2.5.4 Adsorptive Desulfurization	35

<b>CHAPTER</b>	<b>PAGE</b>	
2.5.5	II-Complexation Sorbents	52
2.5.6	Fixed-Bed Adsorption	54
2.6	Inverse Gas Chromatography (IGC) Characterization	56
2.6.1	IGC Theory	56
2.6.2	Topological Index	58
2.7	Previous Studies on the Use of Adsorbents for Selective Sulfur Removal at PPC	59
<b>III</b>	<b>EXPERIMENTAL</b>	<b>61</b>
3.1	Materials	61
3.2	Equipments	63
3.3	Methodology	64
3.3.1	Adsorbents Preparation	64
3.3.2	Reduction	66
3.3.3	Characterization of the Adsorbents	66
3.3.4	Preparation of the Simulated Hydrocarbon Feeds	73
3.3.5	Adsorption of DBT in Toluene on Activated Alumina	73
<b>IV</b>	<b>RESULTS AND DISCUSSION</b>	<b>74</b>
4.1	BET Surface Area, Particle Density, Structural Density and Pore Volume of the Adsorbents	74
4.2	Temperature-Programmed Reduction (TPR) Characterization	75
4.3	Scanning Electron Microscopy (SEM)	78
4.4	X-Ray Diffraction (XRD)	82
4.5	X-Ray Photoelectron Spectroscopy (XPS)	86
4.6	Temperature-Programmed Desorption (TPD) Experiments By Using Thermogravimetric Analysis Coupled with Mass Spectrometer (TGA-MS)	88
4.6.1	Desorption Behavior	88

<b>CHAPTER</b>	<b>PAGE</b>
4.6.2 The Effect of Type of the Adsorbents	91
4.6.3 The Effect of Dispersing Agent on the Metal Dispersion	91
4.6.4 The Effect of Aromatics on Adsorptive Desulfurization	93
4.7 Inverse Gas Chromatography (IGC) Experiments	96
4.7.1 Influence of Injection Volume on the Measurements	96
4.7.2 Enthalpy of Adsorption	99
4.7.3 Free Energy of Adsorption	105
4.7.4 Effect of Adsorption Temperature	108
4.7.5 Surface Free Energy	108
4.7.6 Effect of Type of Adsorbent	114
4.7.7 Effect of Type of Metal Impregnation	116
4.7.8 Effect of Amount of Metal Loading	118
4.7.9 Effect of Dispersing Agent	118
 <b>V CONCLUSIONS AND RECOMMENDATIONS</b>	 120
5.1 Conclusions	120
5.2 Recommendations	121
 <b>REFERENCES</b>	 122
 <b>APPENDICES</b>	 130
<b>Appendix A</b> Sample Preparation Calculations	130
<b>Appendix B</b> Topological Index ( $\chi_T$ ) Calculations	137
<b>Appendix C</b> IGC Characterization Calculations	141
 <b>CURRICULUM VITAE</b>	 158



## LIST OF TABLES

TABLE	PAGE
2.1 Different types of hydrocarbons and their physical and chemical properties	4
2.2 Composition (mol%) and properties of various reservoir fluids and a crude oil	5
2.3 Properties of 21 selected crude oils	6
2.4 Boiling ranges of typical crude oil fractions	8
2.5 True boiling point (TBP) cut points for various crude oil fractions	9
2.6 Destinations for straight-run distillates	11
2.7 Typical compositions of transportation fuels	12
2.8 Clean fuels: limits on sulfur	14
2.9 Physical constants of the principal sulfur compounds	18
2.10 Typical process conditions for hydrotreating different petroleum fractions	23
2.11 Parameters of physical adsorption and chemisorption	36
2.12 Adsorbents in commercial adsorption separations	38
2.13 Pore sizes in typical activated carbon	41
3.1 Properties of activated alumina adsorbents	62
3.2 Physical and chemical properties of chemicals used	62
4.1 Properties of adsorbents characterized by nitrogen adsorption/desorption method at 77 K	74
4.2 Properties of adsorbents by using the Mercury porosimetry	74
4.3 At peak TPR results of 30% Cu/m-Al <sub>2</sub> O <sub>3</sub>	77
4.4 XPS analysis results (reference chemicals) (wt%)	86
4.5 XPS analysis results (wt%)	87
4.6 Adsorption enthalpies ( $-\Delta H_{ads}$ ) (kJ/mol) for the compounds studied over the different adsorbents	103

<b>TABLE</b>	<b>PAGE</b>
4.7 Standard free energy, $-\Delta G_{\text{ads}}$ (kJ/mol), for listed <i>n</i> -alkanes with m-Al <sub>2</sub> O <sub>3</sub> , reduced 30% Cu/m-Al <sub>2</sub> O <sub>3</sub> and M-Al <sub>2</sub> O <sub>3</sub>	107
4.8 $\Delta G_{\text{CH}_2}$ (kJ/mol) at different temperature	110
4.9 Dispersive component of the surface free energy, $\gamma_s^{\text{d}}$ (mJ/m <sup>2</sup> ) at different temperature	110
4.10 Specific interaction, $I^{\text{sp}}$ (mJ/m <sup>2</sup> ) at different temperature (determined by toluene polar probe)	111
4.11 Specific interaction, $I^{\text{sp}}$ (mJ/m <sup>2</sup> ) at different temperature (determined by thiophene polar probe)	111
4.12 The specific interaction ratio of thiophene over toluene on various adsorbents examined by IGC experiments obtained at 200 °C which toluene and thiophene were used as polar probe solutes	113
A1 Physical properties of chemical used in sample preparation step	130
A2 Summary of Adsorbent Preparation Calculations	134
B1 $k_r$ values for different types of bonds	138
C1 Summary of IGC data (an average of retention time, min)	142
C2 Parameters used in calculations (exclusively for reduced 30% Cu/m-Al <sub>2</sub> O <sub>3</sub> adsorbent)	144
C3 Summary of particle density of the adsorbents	147
C4 Physical properties of polar probe molecules (toluene and thiophene) for IGC calculations	154

## LIST OF FIGURES

FIGURE		PAGE
2.1	Sulfur and nitrogen versus API gravity for selected crude oils.	7
2.2	Crude distillation.	8
2.3	Products and composition of Alaska crude oil.	10
2.4	Regulated sulfur levels in diesel fuel in EU, US and Thailand.	13
2.5	Structure of thiophene and its properties.	16
2.6	Structure of benzothiophene and its properties.	16
2.7	Examples of sulfur compounds in petroleum.	19
2.8	GC-FPD chromatograms of gasoline, jet fuel and diesel for identification of sulfur compounds.	20
2.9	Classification of desulfurization processes based on organosulfur compound transformation.	21
2.10	Desulfurization technologies classified by nature of a key process to remove sulfur.	22
2.11	Structures of related polycyclic sulfur compounds found in diesel fuels.	24
2.12	Dependence of reactivity of sulfur compounds versus their ring size and substitution patterns (for sulfur compounds in gasoline, jet fuel and diesel fuel feedstock).	26
2.13	Simulated HDS of diesel to meet 15 and 0.1 ppm level on the basis of a conventional single-stage reactor, assuming 1.0 wt% S in feed; HDS kinetic model: $C_{S, total} = C_{S10} e^{-k1t} + C_{S20} e^{-k2t} + C_{S30} e^{-k3t} + C_{S40} e^{-k4t}$ .	27
2.14	Reaction pathways for dibenzothiophene hydrodesulfurization.	29
2.15	Reaction pathways for 4,6-dimethyldibenzothiophene hydrodesulfurization.	29

<b>FIGURE</b>	<b>PAGE</b>
2.16 Personal vision for research towards comprehensive and effective utilization of hydrocarbon resources in the 21 <sup>st</sup> century.	31
2.17 Concept of proton-exchange membrane fuel cell (PEMFC) system using on-board or on-site fuel processor, or on-board H <sub>2</sub> fuel tank.	32
2.18 Concepts and steps for fuel processing of gaseous, liquid and solid fuels for high-temperature and low-temperature fuel cell applications.	33
2.19 Preparation scheme for precipitated catalyst. Optional preparation steps are indicated by square brackets.	46
2.20 Schematic diagram showing the various steps of a sol-gel process.	48
2.21 Schematic representation for desulfurization of 4,6-DMDBT with molybdenum-based (A) and copper(I)-based (B) adsorbents. Case (B) corresponds to $\pi$ -complexation.	53
2.22 Copper ions occupying faujasite 6-ring windows sites (A); $\sigma$ -donation of $\pi$ -electrons of thiophene to the 4s orbital of copper(I) (B); $d-\pi^*$ backdonation of electrons from 3d orbitals of copper(I) to $\pi^*$ orbitals of thiophene (C). Here 3d represents $d_{xy}$ , $d_{yz}$ or $d_{xz}$ , or 3 of the 53d orbitals.	53
2.23 Means of interaction for a DBT molecule with NiY, corresponding to $\pi$ -complexation.	54
2.24 Idealized breakthrough curve of a fixed-bed adsorber.	54
4.1 Temperature-programmed reduction (TPR) of 30% Cu/m-Al <sub>2</sub> O <sub>3</sub> in 4.95% H <sub>2</sub> in N <sub>2</sub> at 900 °C.	76

<b>FIGURE</b>	<b>PAGE</b>
4.2 SEM images of 30% Cu/m-Al <sub>2</sub> O <sub>3</sub> : (a) cross section of 30% Cu/m-Al <sub>2</sub> O <sub>3</sub> , (b) cluster on the edge of 30% Cu/m-Al <sub>2</sub> O <sub>3</sub> , (c) form of clusters deposited on the surface of 30% Cu/m-Al <sub>2</sub> O <sub>3</sub> .	79
4.3 SEM images of 30% Cu/m-Al <sub>2</sub> O <sub>3</sub> modified with CA with the molar ratio Cu/CA of 10: (a) cross section of 30% Cu/m-Al <sub>2</sub> O <sub>3</sub> modified with CA with the molar ratio Cu/CA of 10, (b) metal occupy the surface, (c) and (d) a “bug chestnut” type cluster.	80
4.4 SEM images of reduced 30% Cu/m-Al <sub>2</sub> O <sub>3</sub> : (a) cross section of reduced 30% Cu/m-Al <sub>2</sub> O <sub>3</sub> , (b) clusters form.	81
4.5 SEM images of reduced 30% Cu/m-Al <sub>2</sub> O <sub>3</sub> modified with CA with the molar ratio Cu/CA of 10: (a) “bug chestnut” typed clusters, (b) a “bug chestnut” type cluster.	81
4.6 Chromatograms of 30% Cu/m-Al <sub>2</sub> O <sub>3</sub> and 30% Cu/m-Al <sub>2</sub> O <sub>3</sub> modified with CA adsorbents.	83
4.7 Diffractograms of CuCl <sub>2</sub> .	83
4.8 Chromatograms of reduced 30% Cu/m-Al <sub>2</sub> O <sub>3</sub> and reduced 30% Cu/m-Al <sub>2</sub> O <sub>3</sub> modified with CA.	84
4.9 Diffractograms of CuCl.	85
4.10 Desorption profiles of pure toluene, 3 wt% DBT in toluene and pure thiophene solutions adsorbed on m-Al <sub>2</sub> O <sub>3</sub> .	89
4.11 Desorption profiles of pure toluene, 3 wt% DBT in toluene and pure thiophene solutions adsorbed on M-Al <sub>2</sub> O <sub>3</sub> .	89
4.12 Desorption profiles of 0, 1, 3 and 5 wt% DBT in toluene adsorbed on m-Al <sub>2</sub> O <sub>3</sub> .	91
4.13 Desorption profiles of pure thiophene solution adsorbed on m-Al <sub>2</sub> O <sub>3</sub> , reduced 30% Cu/m-Al <sub>2</sub> O <sub>3</sub> and reduced 30% Cu/m-Al <sub>2</sub> O <sub>3</sub> modified with CA (Cu/CA=10).	92

FIGURE	PAGE
4.14 Desorption profiles of pure thiophene solution adsorbed on M-Al <sub>2</sub> O <sub>3</sub> , reduced 30% Cu/M-Al <sub>2</sub> O <sub>3</sub> and reduced 30% Cu/M-Al <sub>2</sub> O <sub>3</sub> modified with CA (Cu/CA=10).	92
4.15 Desorption profiles of pure toluene and pure thiophene solutions adsorbed on reduced 30% Cu/m-Al <sub>2</sub> O <sub>3</sub> modified with CA (Cu/CA=10).	94
4.16 Desorption profiles of pure toluene and pure thiophene solutions adsorbed on reduced 30% Cu/M-Al <sub>2</sub> O <sub>3</sub> modified with CA (Cu/CA=10).	94
4.17 Typical gas chromatogram showing output signal following the consecutive injection of <i>n</i> -alkane probes ( <i>n</i> -C <sub>6</sub> – <i>n</i> -C <sub>10</sub> ) and polar probes (toluene and thiophene) at the same acquisition on m-Al <sub>2</sub> O <sub>3</sub> obtained at 225 °C.	97
4.18 specific retention volume as a function of injection volume for <i>n</i> -octane at 250 °C on m-Al <sub>2</sub> O <sub>3</sub> (●), reduced 30% Cu/m-Al <sub>2</sub> O <sub>3</sub> (▲), reduced 30% Cu/m-Al <sub>2</sub> O <sub>3</sub> modified with CA (Cu/CA = 5) (■) and M-Al <sub>2</sub> O <sub>3</sub> (×).	98
4.19 Determination of adsorption enthalpies of non-polar probes ( <i>n</i> -alkanes) on m-Al <sub>2</sub> O <sub>3</sub> at the temperature range between 200–250 °C: hexane (●), heptane (▲), octane (■), nonane (×) and decane (+).	99
4.20 Determination of adsorption enthalpies of non-polar probes ( <i>n</i> -alkanes) on reduced 30% Cu/m-Al <sub>2</sub> O <sub>3</sub> at the temperature range between 200–250 °C: hexane (●), heptane (▲), octane (■), nonane (×) and decane (+).	100

FIGURE	PAGE
4.21 Determination of adsorption enthalpies of non-polar probes ( <i>n</i> -alkanes) on M-Al <sub>2</sub> O <sub>3</sub> at the temperature range between 200–250 °C: hexane (●), heptane (▲), octane (■), nonane (×) and decane (+).	100
4.22 Determination of adsorption enthalpies of polar probes (toluene and thiophene) on m-Al <sub>2</sub> O <sub>3</sub> at the temperature range between 200–250 °C: toluene (◆) and thiophene (▲).	101
4.23 Determination of adsorption enthalpies of polar probes (toluene and thiophene) on reduced 30% Cu/m-Al <sub>2</sub> O <sub>3</sub> at the temperature range between 200–250 °C: toluene (◆) and thiophene (▲).	101
4.24 Determination of adsorption enthalpies of polar probes (toluene and thiophene) on M-Al <sub>2</sub> O <sub>3</sub> at the temperature range between 200–250 °C: toluene (◆) and thiophene (▲).	102
4.25 Adsorption enthalpies of <i>n</i> -alkanes on m-Al <sub>2</sub> O <sub>3</sub> (○), reduced 30% Cu/m-Al <sub>2</sub> O <sub>3</sub> (▲) and M-Al <sub>2</sub> O <sub>3</sub> (□).	103
4.26 Adsorption free energies of <i>n</i> -alkanes on m-Al <sub>2</sub> O <sub>3</sub> (○), reduced 30% Cu/m-Al <sub>2</sub> O <sub>3</sub> (Δ) and M-Al <sub>2</sub> O <sub>3</sub> (□) at 200 °C.	105
4.27 Free energy of different probe adsorptions on m-Al <sub>2</sub> O <sub>3</sub> at different temperatures: 200 °C (●), 225 °C (▲) and 250 °C (■).	106
4.28 Dispersive component of the surface energy, $\gamma_s^d$ , of m-Al <sub>2</sub> O <sub>3</sub> (●) and reduced 30% Cu/m-Al <sub>2</sub> O <sub>3</sub> (▲) as a function of temperature.	109
4.29 Specific interaction, $I^{sp}$ , of m-Al <sub>2</sub> O <sub>3</sub> (●), reduced 30% Cu/m-Al <sub>2</sub> O <sub>3</sub> (▲) and reduced 30% Cu/m-Al <sub>2</sub> O <sub>3</sub> modified with CA (Cu/CA=5) (■) determined by thiophene polar probe as a function of temperature.	112

FIGURE	PAGE
4.30 Specific interaction of toluene and thiophene on both aluminas as a function of temperature: $I^{sp}$ of toluene on m-Al <sub>2</sub> O <sub>3</sub> (○), $I^{sp}$ of toluene on M-Al <sub>2</sub> O <sub>3</sub> (Δ), $I^{sp}$ of thiophene on m-Al <sub>2</sub> O <sub>3</sub> (●) and $I^{sp}$ of thiophene on M-Al <sub>2</sub> O <sub>3</sub> (▲).	114
4.31 Specific interaction of toluene and thiophene on reduced Cu/m-Al <sub>2</sub> O <sub>3</sub> and reduced Cu/M-Al <sub>2</sub> O <sub>3</sub> as a function of metal loading: $I^{sp}$ of toluene reduced Cu/m-Al <sub>2</sub> O <sub>3</sub> (○), $I^{sp}$ of toluene on reduced Cu/M-Al <sub>2</sub> O <sub>3</sub> (Δ), $I^{sp}$ of thiophene on reduced Cu/m-Al <sub>2</sub> O <sub>3</sub> (●) and $I^{sp}$ of thiophene on reduced Cu/M-Al <sub>2</sub> O <sub>3</sub> (▲) obtained at 200 °C.	115
4.32 Specific interaction of toluene on reduced Cu/m-Al <sub>2</sub> O <sub>3</sub> and Ni/m-Al <sub>2</sub> O <sub>3</sub> as a function of metal loading obtained at 200 °C.	117
4.33 Specific interaction of thiophene on reduced Cu/m-Al <sub>2</sub> O <sub>3</sub> and Ni/m-Al <sub>2</sub> O <sub>3</sub> as a function of metal loading obtained at 200 °C.	117
4.34 Specific interaction of toluene and thiophene on reduced 30% Cu/m-Al <sub>2</sub> O <sub>3</sub> and reduced 30% Cu/m-Al <sub>2</sub> O <sub>3</sub> modified with CA (Cu/CA=5) obtained at 200 °C.	119
B1 Graph and matrix <i>D</i> of chloroform.	139
B2 Thiophene structure.	139
C1 $\ln V_g$ against $1/T$ graph of thiophene injected on reduced 30% Cu/m-Al <sub>2</sub> O <sub>3</sub> adsorbent at different temperature ranging between 200–250 °C.	148
C2 Free energy of adsorption of a methylene group based on <i>n</i> -alkanes, 30% Cu/m-Al <sub>2</sub> O <sub>3</sub> adsorbent at 225 °C.	150
C3 Specific interaction parameter, reduced 30% Cu/m-Al <sub>2</sub> O <sub>3</sub> at 225 °C: <i>n</i> -alkanes (continuous line), thiophene (●).	155